Polymer Chemistry

Accepted Manuscript

ROYAL SOCIETY OF CHEMISTRY

www.rsc.org/polymers

Synthesis of nanoscaled poly(styrene-*co*-*n*-butyl acrylate)/silica particles with dumbbell- and snowman-like morphologies by emulsion polymerization

Tatiana Bladé,[a,b,d] *Lucie Malosse,*[b] *Etienne Duguet,*[c] *Muriel Lansalot,*[d]

Elodie Bourgeat-Lami,[d]* *Serge Ravaine* [a]*

[a] CNRS, Univ. Bordeaux, CRPP, UPR 8641, F-33600 Pessac, France.

[b] Manufacture Française des Pneumatiques MICHELIN, 23 place des Carmes Déchaux, 63040 Clermont-Ferrand Cedex 9, France.

[c] CNRS, Univ. Bordeaux, ICMCB, UPR 9048, F-33600 Pessac, France.

[d] Université de Lyon, Univ. Lyon 1, CPE Lyon, CNRS UMR 5265, Laboratoire de Chimie, Catalyse, Polymères et Procédés (C2P2), LCPP group, F-69616 Villeurbanne, France.

* Corresponding authors: bourgeat@lcpp.cpe.fr; ravaine@crpp-bordeaux.cnrs.fr

ABSTRACT

Poly(styrene-*co*-*n*-butyl acrylate) (P(Sty-*co*-BuA)) nanoparticles having diameters in the range of 25-60 nm have been successfully synthesized *via* emulsion polymerization. Sodium styrene sulfonate (SSNa) was used as ionic comonomer, sodium dodecyl sulfate as surfactant and divinyl benzene (DVB) as crosslinking agent. The average polymer particle diameter increased with decreasing the SSNa content in the feed, while increasing DVB concentration increased the size polydispersity. Dumbbell- and snowman-like P(Sty-*co*-BuA)/silica biphasic nanoparticles with silica and polymer nodules smaller than typically 60 nm in diameter were obtained by introducing appropriate amounts of 3-(methacryloxy)propyl trimethoxysilane-functionalized silica nanoparticles as seeds in the emulsion polymerization reaction. Neither the quantity of surfactant nor that of the coupling agent had a strong influence on the obtained morphologies. The control of the number of polymer nodules attached to the silica seed through the modulation of the quantity of silica was also limited, likely because of the low available surface area on each seed in the targeted size range. Consequently, silica/polymer biphasic particles with on average one, two or three polymer nodules at the most were obtained depending on the experimental conditions.

INTRODUCTION

Significant research interests are motivated by the incorporation of inorganic particles into polymer matrices, since it considerably improves their final properties.[1–4] In this sense, fumed silica is considered as a very efficient reinforcing agent of thermoplastic and thermosetting polymers.[5] However, the incompatibility between the highly polar silica surface and the polymer chains, and the formation of aggregates due to surface silanol group interactions via hydrogen bonds make it difficult to achieve optimal use of metal oxide-based fillers in rubber compounds.[6-8] In order to overcome the lack of interactions between non-polar polymer chains and silica surfaces, several strategies have been proposed. Basically they can be divided in two groups based either on the enhancing of physical adsorption of organic molecules on the silica surface, or on the creation of chemical linkages between polymer chains and the silica surface via coupling agent molecules.[9-11] In this context, the synthesis of polymer-silica particles with core-shell, hairy-, multipod- or dumbbell-like morphologies, is a step forward in the compatibilization of highly polar silica surfaces and non-polar polymers.[12-14] Moreover, getting these particles in smaller sizes offers various advantages due to the increased specific surface area. Indeed unique behaviors can emerge when reducing particles size. For instance, Mackay and co- workers,[15] analyzed the miscibility of polymers with nanoparticles in dependence of their relative sizes, and showed that polymeric nanoparticles are completely miscible with a matrix material as long as the particle radius is smaller than the radius of gyration of the polymer matrix. In addition, dissymmetrical particles with distinct hydrophobic and hydrophilic domains can potentially exhibit specific wettability properties and hence, show unusual adsorption behaviors at solid/liquid, liquid/liquid or solid/solid interfaces in comparison to isotropic spherical particles. It was shown in particular that such particles can strongly adsorb at the interface between two immiscible polymer phases and strongly influence the structural evolution of the polymer blends, which in turns

depends on the particle characteristics, such as their aspect ratio, their surface properties and their size. At last the strength of attachment of solid particles to oil/water interfaces is also known to be strongly dependent on the particles size.

Over the past ten years, our group[16-19] and others[20-28] have invested considerable efforts in the synthesis of dumbbell-like polymer/inorganic heterodimers through seeded emulsion polymerization. The ratio between the number of inorganic particles seeds and the number of growing nodules was a key parameter to control the morphology of the final hybrid colloids. However, in these previous works, the diameter of the silica particles was always larger than typically 50 nm and as far as we know, there is no report describing the elaboration of nano-sized dumbbell- or snowman-like silica/polymer heterodimers through heterophase polymerization. One reason may be that the synthesis of such dissymmetrical nanoparticles with very small sizes and a good control of particle morphologies remains a scientific challenge.

The motivation of the present contribution was to synthesize dissymmetrical silica/polymer particles by emulsion polymerization using for the very first time silica seeds smaller than 30 nm. Each particle is expected to be made of one poly(styrene-co-*n*-butyl acrylate) (P(Sty-*co*-BuA)) nodule attached to a single silica sphere, resulting in dumbbell- or snowman-like morphologies depending on the relative sizes of both constituents. The influence of three experimental parameters, *i.e.* the quantities of coupling agent, silica seeds and surfactant, on the morphology of the as-obtained biphasic particles was investigated. Such nanoscaled dissymmetrical particles, which combine the Pickering effect known for particles and the amphiphilic properties of molecular surfactants, could find applications, *e.g.* in the stabilization of fluid interfaces,[29] in the compatibilization of polymer blends[30-32] or as reinforcing fillers, notably for the rubber industry.

EXPERIMENTAL SECTION

Materials. Styrene (Sty, 99+%, Aldrich), sodium 4-styrene sulfonate (SSNa, 90%, Aldrich), divinyl benzene (DVB, 80%, Aldrich) and *n*-butyl acrylate (BuA, 99+%, Aldrich) were used as received. Sodium dodecyl sulfate (SDS, Acros Organic, 99%) was used as surfactant. The initiator, potassium persulfate (KPS, Prolabo), and the coupling agent, 3-(methacryloxy)propyl trimethoxysilane (γ-MPS, 98%, Aldrich) were used without further purification. The aqueous silica sol (Ludox® TM-50) used in this work was purchased from Aldrich (France) as a 50 wt.% colloidal suspension with a number-average particle diameter, D_n, of 27 nm (as determined by TEM), a density (ρ□□□□□□) of 2.3 g cm^{-3} and a specific surface area of 118 m^2 g^{-1} (Table S1 and Figure S1 in the Supporting Information).

Surface modification of the silica seed. Surface grafting of the silica colloids was performed by introducing known amounts of γ-MPS into 1.4 mL of a 250 g L^{-1} stock silica suspension containing 0.5 g L^{-1} of SDS as reported elsewhere.[33] The dispersions were stirred magnetically at ambient temperature and allowed to equilibrate for 4 h. The role of the surfactant was to help the dispersion of the γ-MPS molecules in water and achieve high grafting densities.

Particle synthesis. SDS, water, the monomers (a mixture of Sty and BuA) and the crosslinker (DVB) were introduced in a 1-L glass thermostated reactor fitted with a condenser and purged with nitrogen under stirring (300 rpm) for 60 min before heating to 70 °C. KPS dissolved in 25 mL of deionized water was added to initiate the emulsion polymerization reaction. When present, SSNa was introduced in the water phase before introducing the monomers. The regular withdrawal of samples allowed us to follow the monomer conversion

Table 2. Summary of experimental conditions of the polymerization experiments performed in this study and morphological features of the as-obtained biphasic particles (T = 70 °C).

Run	[Sty] g L^{-1}	[BuA] g L^{-1}	[DVB] g L^{-1}	[SDS] g L^{-1}	[SSNa] g L^{-1}	[KPS] g L^{-1}	[SiO_2] g L^{-1}	[γ-MPS] µmol m^{-2}	Conv. (%)	D_n Latex (nm) [a]	D_w/D_n (TEM)	N_{latex}/N_{silica} *(targeted)*	N_{latex}/N_{silica} *(actual)*	$N_{latex/silica}$
1	10.3	3.3	3	0.5	0.6	0.7	0	-	98	24	1.17	-	-	-
2	12.8		0.2						95	28	1.10	-	-	-
3	12.8	3.3	0.2	0.5	0.6	0.7	35	0	93	31	1.09	0.8	0.6	0
4								0.8	91	31	1.08		0.6	-
5								1.5	98	27	1.11		1	1.1
6								3.3	82	26	1.21		1	-
7								8.3	91	23	1.32		1.5	-
8	12.8	3.3	0.2	0.5	0.6	0.7	70	1.5	98	25	1.03	0.4	0.65	0.9
9							17		99	24	1.33	1.6	3.0	1.1
10							4		94	36	1.10	6.7	3.7	1.9
11							0.4		84	47	1.05	64.0	14.7	2.4
12	12.8	3.3	0.2	0.5	0	0.7	0	-	96	58	1.07	-	-	-
13	43	11	0.5	1.5	0	0.25	0	-	91.5	59	1.02	-	-	-
14	43	11	0.5	1.5	0	0.25	13	0	90	61	1.04	0.8	0.7	0
15								1.5	92	57	1.04		0.9	0.8
16								2.5	83	54	1.05		0.95	-
17								8.3	72[b]	-	-		-	-
18	43	11	0.5	0	0	0.25	13	1.5	18[b]	-	-	-	-	-
19				0.1					32[b]	-	-		-	-
20				0.5					71	60	1.11		0.6	-
21				1					83	57	1.04		0.8	-
22	43	11	0.5	1.5	0	0.25	68	1.5	92	53	1.18	0.15	0.2	0.5
23							45		94	49	1.10	0.2	0.4	0.5
24							4.7		90	57	1.16	2.2	2.4	1.1
25							0.7		91	77	1.27	15.0	6.7	1.9

[a] Size of the P(Sty-co-BuA) nodule determined by TEM. [b] Flocculation occurred.

by gravimetric analysis. When the silane-modified silica seeds were used, they were mixed with the surfactant and the monomers before they were introduced into the reactor. All the experimental conditions of the polymerization experiments performed in this study are displayed in Table 2.

Characterizations. Monomer consumption was followed by gravimetric analysis of samples withdrawn from the polymerization medium at different times. The glass transition temperature (T_g) of the polymer particles was determined by differential scanning calorimetry (DSC). Heat flow from the samples was measured with a DSC Q100 from TA Instruments Waters (USA). The DSC runs were performed at a ramping rate of 10 °C min^{-1} from 0 to 120 °C in aluminum pans that were 7 mm in diameter. For TEM analyses, a drop of the diluted latex suspension was deposited on a carbon-coated copper grid and allowed to evaporate before observation with a Hitachi H600 microscope operating at 70 kV. The number- and weight-average particle diameter (D_n and D_w, respectively) as well as the particle diameter dispersity (D_w/D_n) were determined from the TEM micrographs. The number of latex particles, N_{latex}, was calculated from the monomer-to-polymer conversion and D_n as follows:

$N_{latex} = m_{latex} * \frac{10^{21}}{[(\pi/6)(D_n^3)\rho_{latex}]}$ where m_{latex} (g) is the latex weight, and ρ□□□□□ (1.05 g cm^{-3}) is the latex volumic mass.

The number of silica particles was calculated in a similar way from m_{silica}, ρ_{silica} (2.3 g cm^{-3}) and the silica particle diameter determined by TEM (*e.g.* 27 nm, Table 1).

The targeted N_{latex}/N_{silica} ratio was defined as the ratio of the number of latex particles formed in the absence of silica to the number of silica particles introduced in the reactor. It was compared to the actual N_{latex}/N_{silica} ratio, which is the ratio of the actual number of latex particles formed in the presence of silica to the number of silica particles. Finally the $N_{latex}/_{silica}$ ratio was used to describe particles morphology. It corresponds to the number of

latex particle effectively nucleated around each silica particle, as determined through statistical analysis of the TEM images from at least 200 particles.

RESULTS AND DISCUSSION

Formation of dumbbell-like biphasic particles.

With the goal of preparing dumbbell-like binary particles, we first conducted a series of experiments without any silica seed in order to determine the experimental conditions allowing us to get polymer nanolatexes with a number-average particle diameter close to that of the silica sol, *i.e.*, around 27 nm (Table S1). The reactor was charged with the surfactant, the monomers, KPS and water in the quantities shown in Table 2 (runs 1-2). The monomer composition was fixed such as to reach a glass transition temperature (T_g) close to 65°C (Figure S2 in the Supporting Information) while small amounts of styrene were replaced by DVB in order to partially crosslink the polymer particles. These conditions were selected to form composite particles for use as fillers for rubbery materials. Accordingly, the T_g of the polymer particles was chosen so as to match the viscoelastic properties of the rubbery matrix and to allow for a characterization of the final materials properties at temperatures that remained experimentally accessible both above and below this T_g. The particles also needed to be crosslinked to withstand the mechanical forces imposed by the compounding process. A small quantity of SSNa was also employed as co-monomer to control particles size.

In both cases, stable latexes in the targeted size range were obtained and the monomer-to-polymer conversion was almost complete. We observed an increasing polydispersity of the particle size with increasing DVB concentration (see Supporting Information, Figure S3). This result agrees with the findings reported by Brijmohan *et al.*,[34] and can be attributed to the fact that the swelling capacity of the particles decreases with increasing the crosslinking

degree, which limits particle growth and promotes secondary nucleation. It also cannot be fully ruled out that the oligomers from DVB favor inter-crosslinking between growing particles, which would also contribute to the increased particle size distribution. DVB concentration was thus fixed at 0.2 g L^{-1} for the following seeded-emulsion polymerization experiments.

Effect of γ-MPS grafting density on particle morphology

As shown in previous works, the grafting of a polymerizable silane coupling agent such as γ-MPS is a prerequisite condition for successful formation of biphasic particles made of a central silica core surrounded by polymer nodules.[33,35-36] In order to investigate the influence of this parameter in more depth, a series of polymerization experiments was performed in the presence of un-grafted and γ-MPS-grafted silica suspensions under the experimental conditions given in Table 2 (runs 3-7). The number of introduced silica seeds was close to that of the latex particles expected at the end of the polymerization, *i.e.* N_{latex}/N_{silica} (targeted) = 0.8, in order to favor the formation of dumbbell-like particles. Figure 1 shows the conversion versus time curves for polymerization experiments performed in the presence of silica particles containing an increasing amount of methacryloyloxypropyl groups at their surface. The reaction carried out with bare silica seeds exhibits the same kinetic behavior as that of the reference experiment without silica. The others exhibit a higher polymerization rate, indicating that a high number of polymer particles are formed from the beginning of the polymerization, which suggests that the functionalized silica particles play the role of a seed ensuring the rapid formation of a large number of polymer nanoparticles and accelerating the nucleation process as was previously observed for 80 nm diameter silica particles.[35]

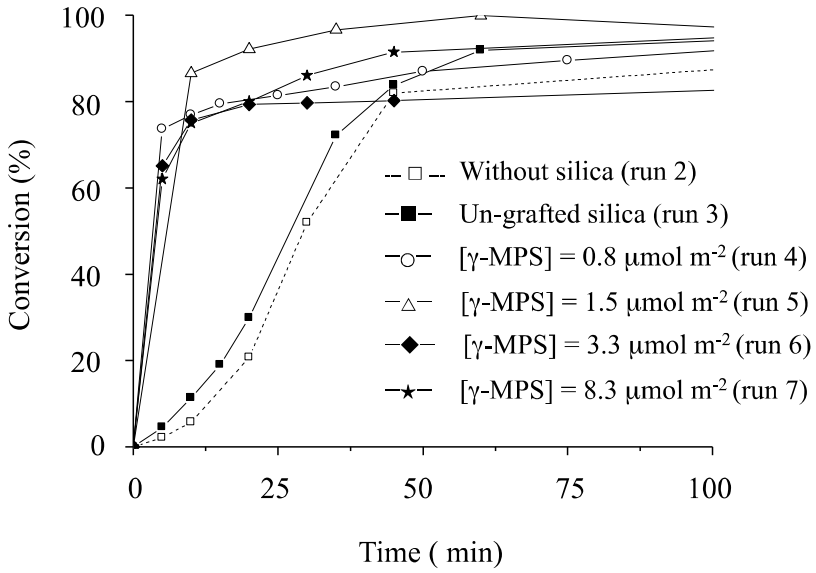

Figure 1. Conversion versus time curves for polymerization experiments performed in the presence of Ludox® TM-50 silica particles with increasing amounts of γ-MPS on their surface. Runs 2-7, Table 2. [Sty] = 12.8 g L^{-1}, [BuA] = 3.3 g L^{-1}, [DVB] = 0.2 g L^{-1}, [SDS] = 0.5 g L^{-1}, [SSNa] = 0.6 g L^{-1}, [KPS] = 0.7 g L^{-1} and [SiO_2] = 35 g L^{-1}.

Figure 2 shows the TEM images obtained for nominal grafting densities of 0 (run 3), 1.5 (run 5) and 8.3 μmol m^{-2} (run 7). It can be seen that the polymerization performed in the presence of non-grafted silica particles gave rise to separate populations of silica beads and polymer latexes with no apparent interactions between them. For the other experiments, the latex spheres showed affinity for the silica surface indicating that the organic modification is mandatory in order to yield biphasic colloids. Particles with a dumbbell-like morphology (the silica and polymer particles having more or less the same size) are mainly produced. Some other biphasic particles resulting from the growth of two latex particles on one silica seed (so-called "trimers", pointed by arrows on TEM pictures) could also be seen.

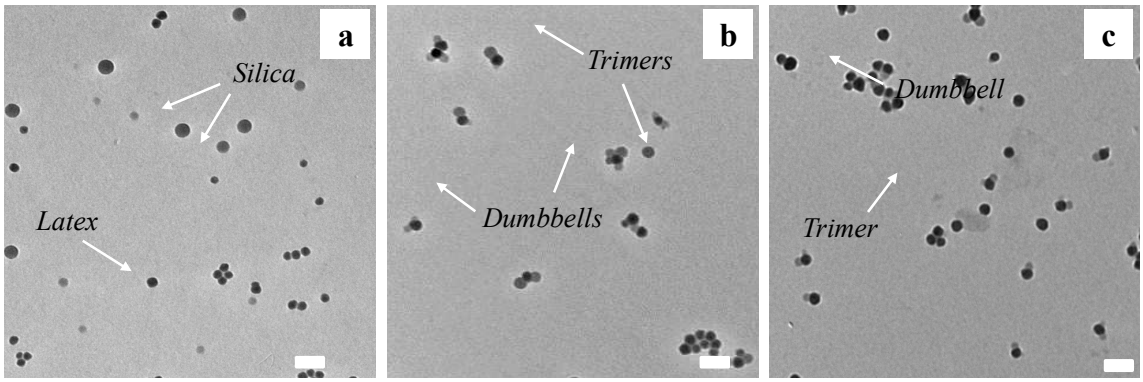

Figure 2. TEM images of Ludox® TM-50 silica/P(Sty-*co*-BuA) particles obtained for different γ-MPS grafting densities: (a) 0 μmol m^{-2} (run 3), (b) 1.5 μmol m^{-2} (run 5), and (c) 8.3 μmol m^{-2} (run 7). Scale bar: 100 nm. [Sty] = 12.8 g L^{-1}, [BuA] = 3.3 g L^{-1}, [DVB] = 0.2 g L^{-1}, [SDS] = 0.5 g L^{-1}, [SSNa] = 0.6 g L^{-1}, [KPS] = 0.7 g L^{-1} and [SiO_2] = 35 g L^{-1}.

The particle size and size distribution of the P(Sty-*co*-BuA) latexes directly determined from the TEM micrographs as a function of the γ-MPS grafting density are summarized in Table 2 (runs 3-7). It can be seen that the diameter of the copolymer latex particles decreases with increasing the γ-MPS grafting density, suggesting that silica particles with increasing amounts of methacryloyloxypropyl groups at their surface, are capable of stabilizing a greater number of latex particles as previously reported in the literature for larger silica particles.[35] Consequently, the actual N_{latex}/N_{silica} ratio increased and was getting farther away from the targeted value. The $N_{latex/silica}$ ratio evolved in a similar way and a majority of dumbbell-shaped particles were obtained for nominal grafting densities of 1.5 or 3.3 μmol m^{-2}. However, surprisingly, this last parameter did not have a significant influence on particle morphology contrary to the results previously reported for larger silica particles.[33] Indeed, multipod-like particles were formed whatever the γ-MPS grafting density with a number of polymer nodules not exceeding 1.5. This may be related to the small diameter of the silica seed and the associated small surface area that does not allow the growth of a large number of polymer nodules.

Effect of the silica concentration

A series of experiments was performed with increasing silica concentrations and under the conditions listed in Table 2 (runs 8-11) in order to verify whether the $N_{latex/silica}$ ratio could be effectively controlled by adjusting the targeted N_{latex}/N_{silica} ratio as shown previously for emulsion polymerization of styrene in the presence of larger silica seeds.[37-38] The results obtained in the present work demonstrated that this parameter is also pertinent, but less accurate. Actually, it can be seen in Table 2 that the diameter of the latexes increased with decreasing the silica concentration, *i.e.* with increasing N_{latex}/N_{silica}. The overall number of latex particles thus decreased leading to an increasing discrepancy between the actual and targeted N_{latex}/N_{silica} ratios. This result highlights once again the importance of the silica particles seed in controlling polymer particles nucleation. More precisely, Figures 3 and Table 2 show that dumbbell-like particles ($N_{latex/silica} = 1$) are mainly obtained when $N_{latex}/N_{silica} \leq 2$. Figure 4 shows the relative proportions of the various morphologies observed for the biphasic particles for different N_{latex}/N_{silica} ratios, calculated by a statistical analysis based on 200 particles for each experiment. It is seen that when higher N_{latex}/N_{silica} ratios were targeted, the observed $N_{latex/silica}$ differed from the expected values. For instance, in Figure 3e ($N_{latex}/N_{silica} = 64$) a complex mixture of dumbbell-like, trimers, tetramers (one silica surrounded by three polymer nodules) was observed, while particles containing more than 3 polymer nodules were scarce. In these situations, the small contact angle of the P(Sty-*co*-BuA) nodules with the silica surface was not favorable to the coexistence of several copolymer nodules, because the available surface area on each seed was low. In addition, one should also note that the proportion of free latex particles increased while increasing N_{latex}/N_{silica} as expected. Indeed, the lower the silica concentration, the lower the probability of free radical capture by silica and the higher the extent of secondary nucleation. In summary, the highest proportion of

dumbbell-like particles (i.e. 54 and 48%, respectively) was achieved for targeted N_{latex}/N_{silica} ratios close to one while decreasing the silica concentration (i.e. increasing N_{latex}/N_{silica}) promoted secondary nucleation.

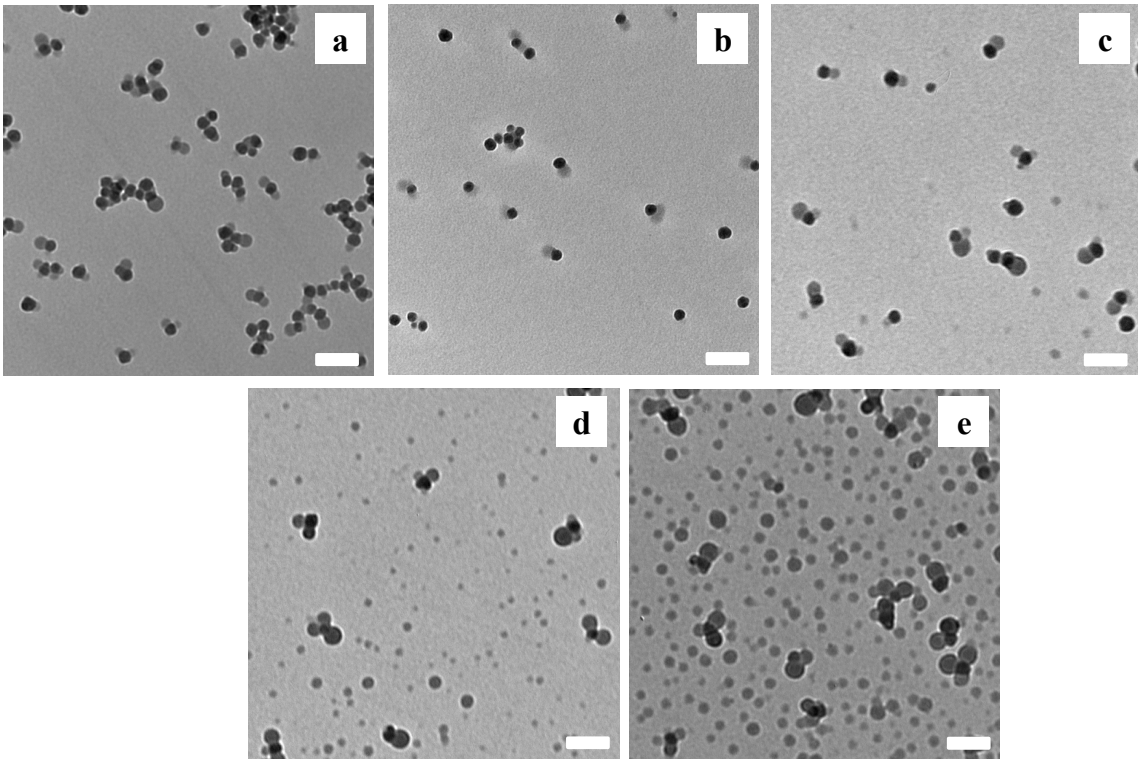

Figure 3. TEM images of Ludox® TM-50 silica/P(Sty-*co*-BuA) biphasic particles obtained for different N_{latex}/N_{silica} ratios: (a) 0.4 (run 8), (b) 0.8 (run 5), (c) 1.6 (run 9), (d) 6.7 (run 10) and (e) 64 (run 11). Scale bar: 100 nm. [Sty] = 12.8 g L^{-1}, [BuA] = 3.3 g L^{-1}, [DVB] = 0.2 g L^{-1}, [SDS] = 0.5 g L^{-1}, [SSNa] = 0.6 g L^{-1}, [KPS] = 0.7 g L^{-1} and [γ-MPS] = 1.5 μmol m^{-2}.

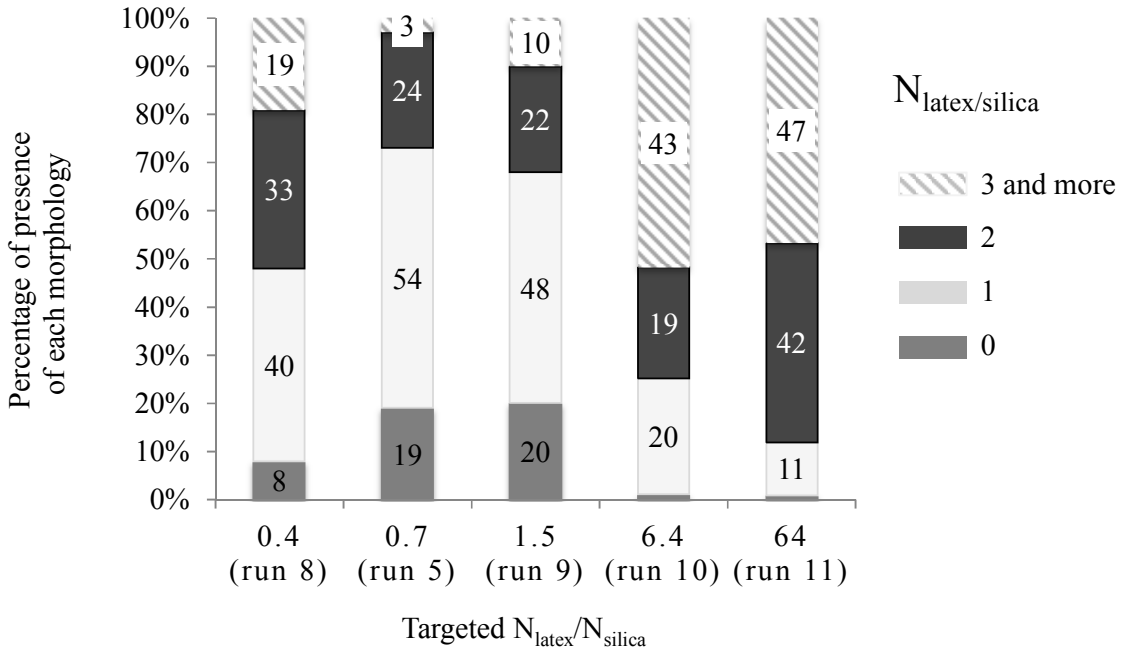

Figure 4. Relative proportions of the different morphologies ($N_{latex/silica}$) observed in batches of Ludox® TM-50 silica/P(Sty-*co*-BuA) biphasic particles obtained for different targeted N_{latex}/N_{silica} ratios, as determined by statistical analysis of TEM images. [Sty] = 12.8 g L^{-1}, [BuA] = 3.3 g L^{-1}, [DVB] = 0.2 g L^{-1}, [SDS] = 0.5 g L^{-1}, [SSNa] = 0.6 g L^{-1}, [KPS] = 0.7 g L^{-1} and [γ-MPS] = 1.5 μmol m^{-2}.

Formation of snowman-like biphasic particles.

Our second goal was to synthesize snowman-like particles whose silica part would be smaller than the organic nodule. We thus first performed another series of experiments without any silica seed in order to determine the experimental conditions leading to nanolatexes with a number-average particle diameter larger than 30 nm. By comparison with run 2 in the previous series of experiments (Table 2), we did not use SSNa as comonomer in order to reduce the number of anionic charges at the particle surface, and hence, form larger particles (run 12, Table 2). A stable latex with a number-average particle diameter of 58 nm was obtained. We also performed a similar experiment multiplying the amounts of styrene

and BuA by ~3.3 to increase the solid content up to 5 wt. % but it then was necessary to decrease the amount of initiator and to multiply the SDS concentration by three (run 13, Table 2) to get a stable latex suspension with a number-average particle diameter of 59 nm (see Supporting Information, Figure S4). It is worth noting that polymerization experiments performed with SDS concentrations lower than typically 1.5 g L^{-1} systematically yield unstable latexes.

Effect of the γ-MPS grafting density on particle morphology

We next performed a series of polymerization experiments in the presence of un-grafted and γ-MPS-grafted silica suspensions under the conditions of run 13, as listed in Table 2 (runs 14-17). The amount of silica was fixed such as N_{latex}/N_{silica} = 0.8 in order to promote the growth of only one polymer nodule onto one silica seed and thus to avoid the formation of trimers and tetramers. Figure 5 shows the TEM images of the obtained biphasic particles for grafting densities of 0, 1.5 and 2.5 µmol m^{-2}. As previously, the polymerization performed in the presence of non-grafted silica particles gave rise to separate populations of silica beads and polymer latexes with no apparent interaction between them. For low γ-MPS grafting densities (≤ 2.5 µmol m^{-2}), particles with a snowman-like morphology were mainly produced. Some free silica seeds and polymer particles could also be seen. When the γ-MPS grafting density increased to *ca.* 8.3 µmol m^{-2}, the conversion was limited to *ca.* 72 %, the latex becoming unstable, preventing any reliable statistical analysis. This is probably due to the high affinity of the growing latex for the modified silica surface, which favors the agglomeration of the particles through the encapsulation of several silica seeds within a larger polymer particle.

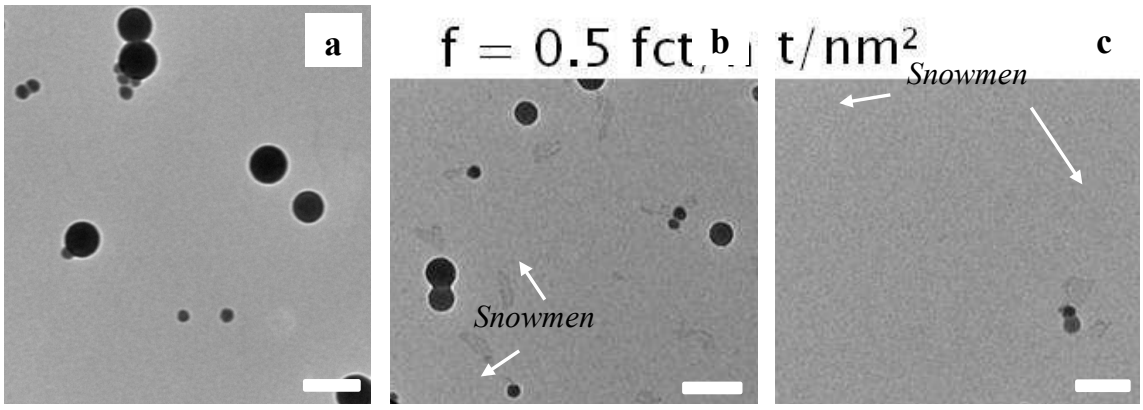

Figure 5. TEM images of Ludox® TM-50 silica/P(Sty-co-BuA) biphasic particles obtained for different γ-MPS grafting densities: (a) 0 µmol.m^{-2} (run 14), (b) 1.5 µmol m^{-2} (run 15) and (c) 2.5 µmol m^{-2} (run 16). Scale bar: 100 nm. [Sty] = 43 g L^{-1}, [BuA] = 11 g L^{-1}, [DVB] = 0.5 g L^{-1}, [SDS] = 1.5 g L^{-1}, [KPS] = 0.25 g L^{-1} and [SiO_2] = 13 g L^{-1}.

Effect of the SDS concentration

As mentioned previously, polymerization experiments performed in absence of silica seeds gave stable latexes only if the concentration of SDS was larger than 1.5 g L^{-1} (run 13, Table 2). We studied the influence of this parameter when γ-MPS-grafted silica nanoparticles ([γ-MPS] = 1.5 µmol m^{-2}) were introduced in the reaction medium (runs 18-21, Table 2). Figure 6 shows the conversion versus time curves for polymerization experiments performed in the presence of various amounts of surfactant. When [SDS] increased, both conversion and polymerization rate increased as expected since the surfactant molecules are able to stabilize more growing polymer particles. When [SDS] was lower than 0.5 g L^{-1}, the conversion was very low and the latex became quickly unstable. However, the conversion was almost complete when [SDS] = 1 g L^{-1} (which was not the case in the absence of silica nanoparticles), confirming that the functionalized silica seeds are also able to stabilize the growing polymer nanoparticles. In that case, snowman-like particles whose polymer nodules were slightly larger than those of particles formed when [SDS] = 1.5 g L^{-1} were obtained, as expected (Supporting Information, Figure S5).

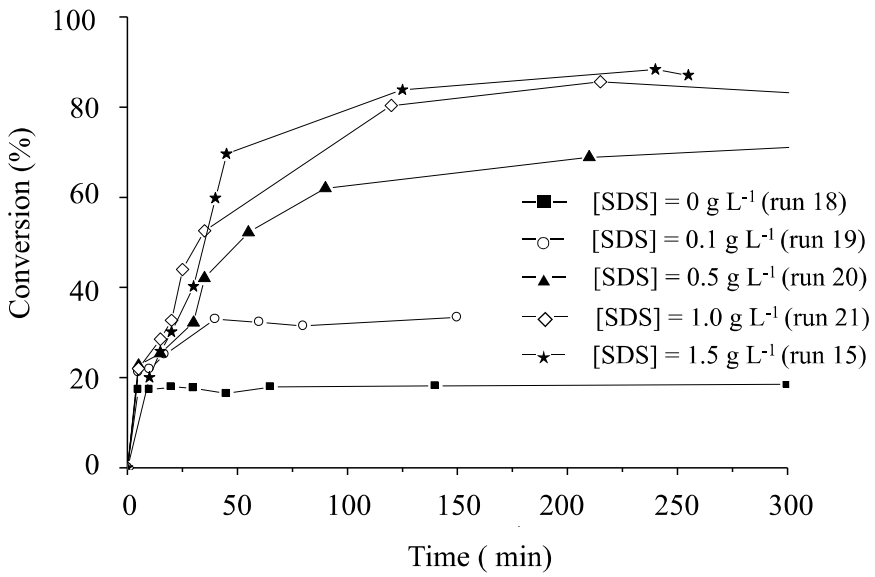

Figure 6. Conversion versus time curves for polymerization experiments performed in the presence of Ludox® TM-50 silica particles and increasing amounts of SDS. [Sty] = 43 g L^{-1}, [BuA] = 11 g L^{-1}, [DVB] = 0.5 g L^{-1}, [γ-MPS] = 1.5 μmol m^{-2}, [KPS] = 0.25 g L^{-1} and [SiO_2] = 13 g L^{-1}.

Effect of the silica concentration

We also studied the influence of the N_{latex}/N_{silica} ratio on the morphology of the composite particles by running a series of experiments with increasing silica concentrations as listed in Table 2 (runs 22-25). When $N_{latex}/N_{silica} \leq 1$, snowman-like particles and free silica seeds were observed (Figure 7). A statistical analysis showed that the proportions of trimers and tetramers increased when N_{latex}/N_{silica} was larger than one (Figure 8). As previously, the observed $N_{latex/silica}$ ratio was lower than the expected value, indicating that the growing polymer nodules either coalesced or were expulsed from the seed, its surface area being too low for allowing a high number of attached nodules to grow independently.

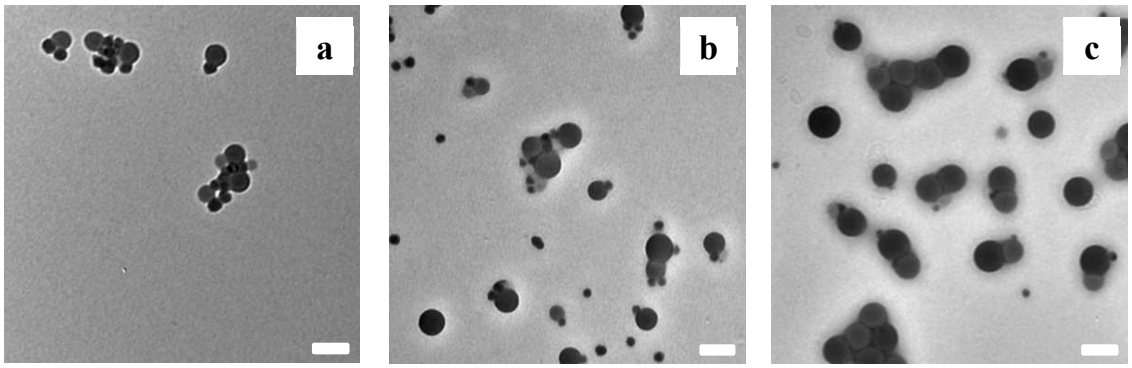

Figure 7. TEM images of Ludox® TM-50 silica/P(Sty-co-BuA) biphasic particles obtained for different N_{latex}/N_{silica} ratios: (a) 0.2 (run 23), (b) 2.2 (run 24) and (c) 15.0 (run 25). Scale bar: 100 nm. [Sty] = 43 g L^{-1}, [BuA] = 11 g L^{-1}, [DVB] = 0.5 g L^{-1}, [SDS] = 1.5 g L^{-1}, [γ-MPS] = 1.5 μmol m^{-2} and [KPS] = 0.25 g L^{-1}.

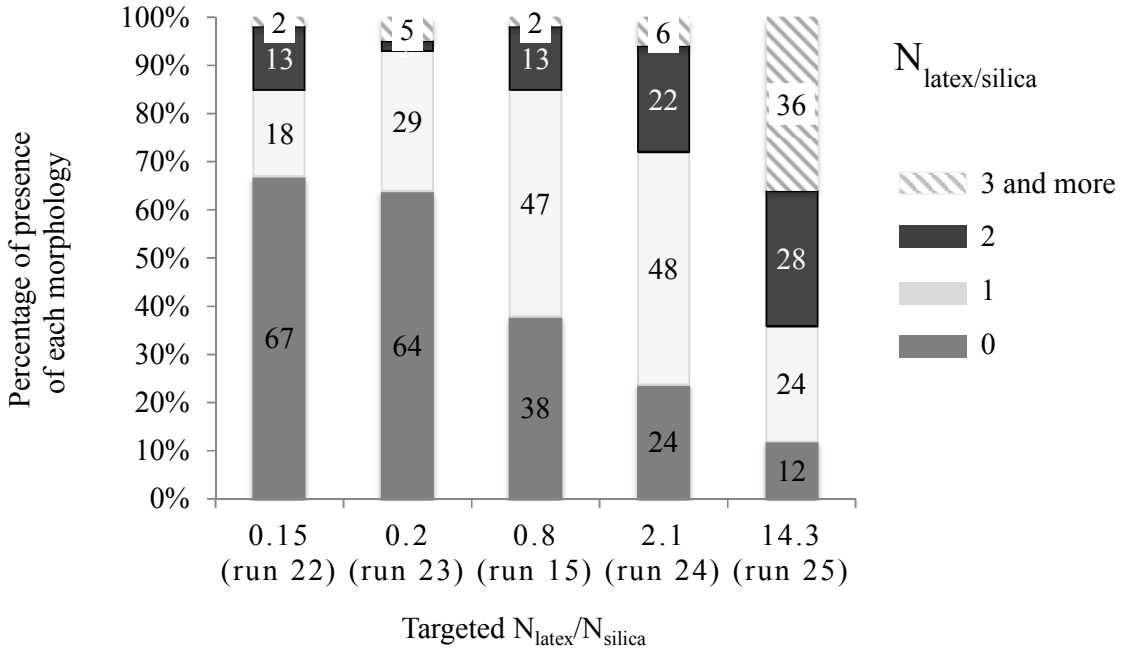

Figure 8. Relative proportions of biphasic particles ($N_{latex/silica}$) obtained for different N_{latex}/N_{silica} ratios, as determined by statistical analysis of TEM images. [Sty] = 43 g L^{-1}, [BuA] = 11 g L^{-1}, [DVB] = 0.5 g L^{-1}, [SDS] = 1.5 g L^{-1}, [γ-MPS] = 1.5 μmol m^{-2} and [KPS] = 0.25 g L^{-1}.

CONCLUSIONS

Silica/P(Sty-*co*-BuA) biphasic nanoparticles were synthesized under batch emulsion polymerization. The silica seeds, whose surface was modified through the grafting of γ-MPS molecules, were able to stabilize the growing latex particles and induced an acceleration of the polymerization kinetics. Particles with dumbbell-like and snowman-like morphologies were preferentially obtained when N_{latex}/N_{silica} was ≤ 1. When higher N_{latex}/N_{silica} ratios were used, the observed $N_{latex/silica}$ did not match the expected values because the available surface area on each seed was too low to capture all nucleated latex particles and/or to accommodate a high number of P(Sty-*co*-BuA) nodules.

SUPPORTING INFORMATION

Main characteristics and TEM image of the Ludox® TM-50 colloidal silica particles. DSC thermogramm of run 2. TEM images of the latexes obtained in runs 1, 2, 13 and 21, respectively.

ACKNOWLEDGMENTS

The Michelin Company is gratefully acknowledged for the PhD scholarship of Dr Tatiana Bladé.

REFERENCES

1 C. C. Sun and J. E. Mark, *Polymer*, 1989, **30**, 104–106.

2 Y. Ikeda and S. Kohjiya, *Polymer*, 1997, **38**, 4417–4423.

3 M. J. Wang, *Rubber Chem. Technol*., 1998, **71**, 520–589.

4 J. B. Donnet, *Rubber Chem. Technol*., 1998, **71**, 323–341.

5 A. Camenzind, W. R. Caseri and S. E. Pratsinis, *Nano Today*, 2010, **5**, 48–65.

6 S. Wolff and M.-J. Wang, *Rubber Chem. Technol*., 1992, **65**, 329–342.

7 Y. Li, M. J. Wang, T. Zhang, F. Zhang and X. Fu, *Rubber Chem. Technol*., 1994, **67**, 693–699.

8 N. Suzuki, M. Ito and S. Ono, *J. Appl. Polym. Sci*., 2005, **95**, 74–81.

9 V. V. Kazakova, A. S. Zhiltsov, O. B. Gorbatsevitch, I. B. Meshkov, M. V. Pletneva, N. V. Demchenko, G. V. Cherkaev and A. M. Muzafarov, *J. Inorg. Organomet. Polym*., 2012, **3**, 564-576.

10 J. Lopez Valentín, A. Rodríguez Díaz, L. Ibarra Rueda and L. Gonzalez Hernandez, *J. Appl. Polym. Sci*., 2004, **91**, 1489–1493.

11 M. N. Tchoul, M. Dalton, L.-S. Tan, H. Dong, C. M. Hui, K. Matyjaszewski and R. A. Vaia, *Polymer*, 2012, **53**, 79-86.

12 S. Chuayjuljit and A. Boonmahitthisud, *Appl. Surf. Sci*., 2010, **256**, 7211-7216.

13 I. Mora-Barrantes, J. L. Valentín, A. Rodríguez, I. Quijada-Garrido and R. Paris, *J. Mater. Chem*., 2012, **22**, 1403-1410.

14 E. Chabert, M. Bornert, E. Bourgeat-Lami, J-Y. Cavaillé, R. Dendievel, C. Gauthier, J-L. Putaux, A. Zaoui, *Mater. Sci. Eng. A*, 2004, **381**, 320-330.

15 M. E. Mackay, A. Tuteja, P. M. Duxbury, C. J. Hawker, B. Van Horn, Z. Guan, G. Chen and R. S. Krishnan, *Science* 2006**, 311***,* 1740–1743.

16 S. Reculusa, C. Poncet-Legrand, A. Perro, E. Duguet, E. Bourgeat-Lami, C. Mingotaud and S. Ravaine, *Chem. Mater*., 2005, **17**, 3338-3344.

17 A. Perro, S. Reculusa, F. Pereira, M-H. Delville, C. Mingotaud, E. Duguet, E. Bourgeat-Lami and S. Ravaine, *Chem. Commun*., 2005, 5542-5543.

18 A. Perro, S. Reculusa, E. Bourgeat-Lami, E. Duguet and S. Ravaine, *Colloid Surf. A-Physicochem. Eng. Asp.*, 2006, **284**, 78-83.

19 J. Parvole, I. Chaduc, K. Ako, O. Spalla, A. Thill, S. Ravaine, E. Duguet, M. Lansalot and E. Bourgeat-Lami, *Macromolecules*, 2012, **45**, 7009-7018.

20 W. Qiang, Y. Wang, P. He, H. Xu, H. Gu and D. Shi, *Langmuir* 2008, **24**, 606-608.

21 D. Nagao, M. Hashimoto, K. Hayasaka and M. Konno, *Macromol. Rapid Commun.* 2008, **29**, 1484–1488.

22 W. Lu, M. Chen and L. Wu, *J. Colloid Interf. Sci.* 2008, **328**, 98-102.

23 A. Ohnuma, E. C. Cho, P. H. C. Camargo, L. Au, B. Ohtani and Y. Xia, *J. Am. Chem. Soc.* 2009, **131**, 1352-1353.

24 B. M. Teo, S. K. Suh, T. A. Hatton, M. Ashokkumar and F. Grieser, Langmuir 2011, **27**, 30-33.

25 Y. Yin, S. Zhou, B. You and L. Wu, *J. Polymer Sci. Part A. Polym. Chem.* 2011, **49**, 3272-3279.

26 D. Nagao, M. Sugimoto, A. Okada, H. Ishii, M. Konno, A. Imhof and A. van Blaaderen, *Langmuir* 2012, **28**, 6546–6550.

27 N. Shibata, D. Nagao, H. Ishii, and M. Konno, *Colloid Polym. Sci.* 2013, **291**, 137–142.

28 X. Ji, M. Wang, X. Ge and H. Liu, Langmuir 2013, **29**, 1010-1016.

29 F. Tu, B. J. Park and D. Lee, *Langmuir*, 2013, **29**, 12679-12687.

30 J. Vermant, G. Cioccolo, K. G. Nair and P. Moldenaers, *Rheologica Acta*, 2004, **43**, 529-538.

31 A. Walther, K. Matussek and A. H. E. Müller, *ACS Nano*, 2008, **2**, 1167-1178.

32 M. Huang and H. Guo, Soft Matter, 2013, **9**, 7356-7368.

33 E. Bourgeat-Lami, M. Insulaire, S. Reculusa, A. Perro, S. Ravaine and E. Duguet, *J. Nanosci. Nanotechnol*. 2006, **6**, 432-444.

34 S. B. Brijmohan, S. Swier, R. A. Weiss and M. T. Shaw, *Ind. Eng. Chem. Res*., 2005, **44**, 8039–8045.

35 E. Bourgeat-Lami, N. Negrete Herrera, J.-L. Putaux, S. Reculusa, A. Perro, S. Ravaine, C. Mingotaud and E. Duguet, *Macromol. Symp*., 2005, **229**, 32-46.

36 E. Bourgeat-Lami, N. Negrete Herrera, J.-L. Putaux, S. Reculusa, A. Perro, S. Ravaine and E. Duguet, *Macromol. Symp*., 2007, **248**, 213-226.

37 A. Perro, E. Duguet, O. Lambert, J.-C. Taveau, E. Bourgeat-Lami and S. Ravaine, *Angew. Chem. Int. Ed*., 2009, **48**, 361-365.

38 A. Désert, I. Chaduc, S. Fouilloux, J.-C. Taveau, O. Lambert, M. Lansalot, E. Bourgeat-Lami, A. Thill, O. Spalla, S. Ravaine and E. Duguet, *Polym. Chem*., 2012, **3**, 1130-1132.

TOC GRAPHIC